CAMERA CALIBRATION FOR STEREO P.I.V. WITH A FRONT-REAR CAMERA ARRANGEMENT. APPLICATION TO OPEN-CHANNEL FLOW.

J. C. WELLS[1], H. SUGIMOTO[2], C.V. NGUYEN[3], K. KISHIDA[4]

[1]Member JSCE, Ph.D., Associate Professor, Dept. of Civil & Environmental Systems Engineering
[2]Machining Instructor; [3]Graduate School of Science and Engineering; [4]Postdoctoral Fellow

Faculty of Science & Engineering, Ritsumeikan University (Noji Higashi 1-1-1, Kusatsu, Shiga 525-8577 Japan)

We perform high-resolution stereo P.I.V. at 15 *Hz* in a cross-stream plane in the lower half of a smooth-bed open channel flow at $Re_\tau = u_\tau h / \nu = 300$. This paper describes technical details of our system, concentrating on questions of calibration and validation. We demonstrate theoretically and experimentally that the pinhole model may by applied without modification to a Scheimpflug camera, and present a calibration target designed for Willert's "front-and-rear" stereo camera arrangement. A cross-check on the two horizontal components of instantaneous velocity vectors, using a third camera viewing from below with beam illumination (rather than sheet illumination), gives good agreement with results from stereo P.I.V.

Key Words : *turbulent flow, open channel, streamwise vortex, stereo particle image velocimetry*

1. INTRODUCTION

Based on DNS data, Stretch[1)] proposed a staggered typical arrangement of streamwise vortices ("SV") in turbulent channel flow (cf. Jeong *et al.*[2)]). In previous work by our group, high-resolution videographic P.I.V., with illumination in the cross-stream plane, was applied to measure the two cross-stream components of velocity at 15 *Hz* and 1 *Hz* in the lower half of a smooth-bed open channel flow at $Re_\tau = u_\tau h / \nu = 300$ (h: flow depth = 10.0 *cm*; width 50 *cm*; 5.5 *m* from channel entrance). Based on such measurements, and on dye visualizations, we claimed (Wells *et al.*, [3),4)]) to provide the first direct experimental evidence for Stretch's staggered arrangement of SV. Wells & Yamamoto [5)] presented spatio-temporal correlations associated with SV structure, and considers the relationship between vortex cores and their associated straining regions.

In the present communication, we apply time-resolved *stereo* PIV (hereafter, "SPIV") in the cross-stream plane under similar experimental conditions; since all three velocity components are now measured, this technique permits us to investigate the relationship of streamwise vortices with lifted slow-speed streaks and with regions of high *-uv*. Our 3D velocity data, as visualized in "quasi-3D" by application of Taylor's hypothesis, appear very realistic, and average velocity profiles agree quite well with two-component ("2C") PIV data in the cross-stream and streamwise-vertical planes[6)]. However our validation thus far has been limited to *average* statistics, and indeed there appears to be some error in the spanwise component of velocity; the average spanwise component is measured to be 1% of the average streamwise velocity, while 2C-PIV with one camera viewing from directly downstream suggests that the average spanwise component is at most 1/10 of that value. Thus we view our present data as preliminary. We are now using a third digital camera to view the measurement station from below; this permits direct validation of the two horizontal components of *instantaneous* velocity vectors, as detailed later.

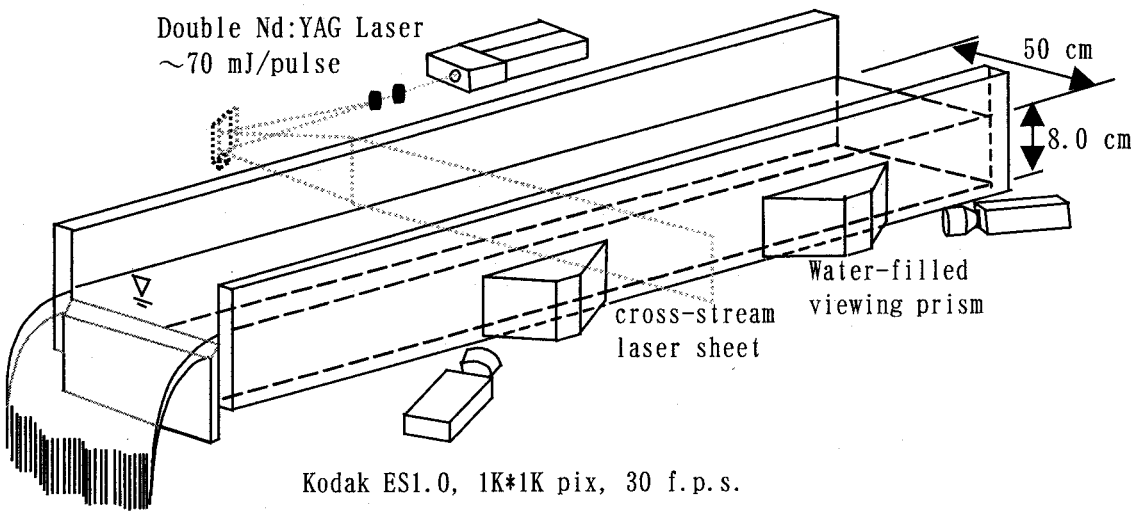

Fig. 1. Perspective view of stereo PIV arrangement. Camera 3, discussed in section 3, views the measuring station from below through the glass bottom of the channel.

Organization of the paper. Section 2 describes our method and apparatus, emphasizing our novel calibration target, and application of the pinhole camera model to the Scheimpflug arrangement. Section 3 describes the cross-check with the third camera; Section 4 offers a summary and outlook.

2. METHOD

We have performed stereo particle image velocimetry ("SPIV") in smooth-bed open channel flow at $Re_\tau = u_\tau h / \nu = 300$, equivalent to a bulk flow Reynolds number of $U h / \nu = 5250$. Flow depth d is 8.0 *cm*. The channel width and length are respectively 50 *cm* and 7.5 *m*. A 3 *mm* thick double-pulsed laser sheet is produced by a double Nd-YAG laser run at 15 *Hz*, illuminating a cross-stream plane 5.2 *m* from the channel entrance, with an interval between pulses of Δt = 5 ms and synchronized so as to straddle pairs of video images recorded at 30 *Hz* by two Kodak ES1.0 progressive-scan cameras; velocity fields are thus obtained at 15 *Hz*. Image resolution is 1K×1K, and Nikkor 105 *mm* microlenses are used with an f-number of 5.8 or greater. The field of view is 5.0 *cm* wide×4.5 *cm* high, so that only the lower half of the channel is observed. Near-neutrally buoyant hollow glass spheres (Sphericel™ powder, Potters Industries, USA), sieved to remove particles less than 10μm in diameter and thus lying in the range of diameters of 10-15 μm, serve as flow tracers. Velocity components are calculated by maximizing the normalized cross-correlation of 49×49 pixel templates between image pairs. In our past 2D PIV work with a single camera under otherwise similar conditions, tests with a rotating plate of transparent plastic modeling the tracer-laden fluid showed that streamwise vorticity could be estimated with acceptable accuracy by first smoothing velocity vectors with the 8 surrounding values.

To image the entire field of view in focus as per the Scheimpflug condition, the camera body is mounted on an angular stage whose axis of rotation passes vertically through the center of the CCD sensor. The body angle is adjusted while viewing the image until optimal focus is achieved; this angle is about 5 degrees from the lens axis in our case. Following Willert[7], the cameras look symmetrically from opposite sides of the light sheet (Fig. 1) such that light is forward-scattered, with accordingly high and equal intensity, to both cameras. Water-filled viewing prisms minimize refraction at the air-glass-water interface. If the cameras are symmetrically positioned, a second advantage of this front-and-rear camera arrangement is that image distortion is symmetric for the two cameras. Thus registration errors, *i.e.* mismatching of corresponding points from the two camera views, can be eliminated if reference points are accurately registered.

(1) Calibration Target

Soloff *et al.*[8] state "the design of the calibration target is the most important part of performing successful calibration." A standard calibration protocol, one used by Soloff *et al.*, is to take a series of photographs of a planar calibration target, typically a rectangular grid of reference points oriented parallel to the light sheet, as the target is stepped through several positions in the direction normal to the sheet. However, our experience with this method has not been very satisfying. One practical difficulty is to conveniently and accurately orient the rather small (~ 5 *cm* $\times 5$ *cm*) surface of the calibration target and the axis of the translation stage, say to within 10^{-4} radians, for which purpose one requires large reference surfaces. Second, even if the target can be oriented accurately, one wants

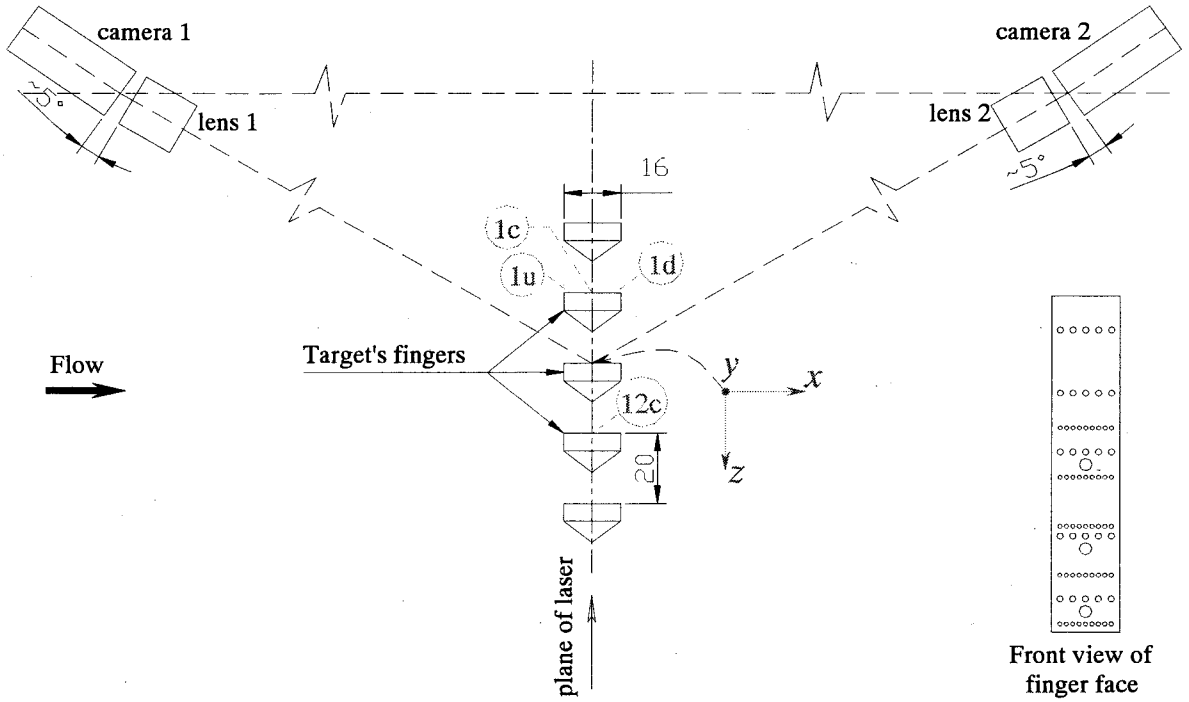

Fig. 2 Schematic of calibration target in plan view and definition of coordinate system; inset to right shows arrangement of reference points (largest circles are screw heads). The positions of the reference points shown in Fig 3 are indicated for comparison.

reproducible positioning to avoid time-consuming adjustments before each new experimental trial. Finally, in the present camera arrangement, we would like a target which can be viewed from both sides of the light sheet. The standard solution to this requirement would be to sandwich, between two glass plates, an overhead transparency sheet on which a grid of reference points is printed. Again, our experience with this method was disappointing; the laser printers we tried were all sufficiently imprecise as to produce visibly curved grid lines. Also, there is a slight error introduced by mismatched refractive indices between glass and water.

For these reasons, we made a target with a *three-dimensional pattern* of reference points located on five vertical "fingers" whose 16 *mm*-wide faces lie in streamwise-vertical planes facing the camera side of the channel, and on which horizontal rows of reference points were machined with a vertical end-mill to a precision of +/- 5 μm at various heights. The fingers are spaced at 20 *mm* intervals in the span direction; their backs beveled to allow the cameras a clear view of the finger behind (Fig. 2), and are attached to a 60 *cm* long superstructure oriented in the stream direction. Two complementary calibration patterns were machined, one with reference points 1000 μm in diameter at a horizontal spacing (in the stream direction) of 3000 μm, the other with 300 μm diameter points spaced at 1500 μm intervals. The former are easier to find, and might be used for future experiments with a larger field of view, while the latter allow precise subpixel search and were used for the trials reported here. Fig. 3 shows an example of a calibration photograph for the present experiments, in which only three fingers fit into the field of view. The largest marks are screw heads painted white; these are easily found in a preliminary pass of the reference point search procedure, and the actual reference points are then located by searching small regions shifted suitably from the screw heads. A 60 *cm*-long surface of the superstructure is used for orientation about the vertical axis, while orientation around the two horizontal axes is adjusted so as to simultaneously bring point gages at three extremities of the superstructure into contact with a static water surface. The superstructure is attached to a vertical stage with three linear bearings having a 20 *cm* stroke, allowing convenient and precise repositioning of the target.

In principle the same kind of calibration target could be applied to the standard SPIV arrangement with both cameras on the same side of the laser sheet; then parallel faces with reference marks would be required on both sides of the fingers (imagine eliminating the triangular beveled backs in Fig 2.). It should be noted however that the reference points seen by one camera would be hidden from the other, and it is not obvious how to mark both sides of each finger, and then assemble the fingers, with enough precision to eliminate registration errors.

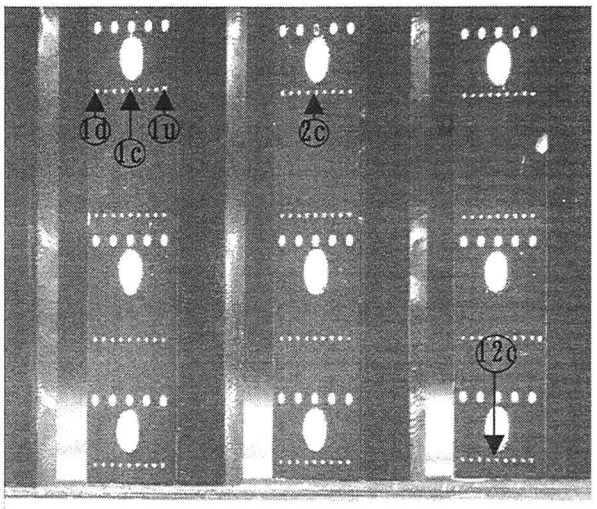

Fig. 3 Photograph of calibration target from camera 1 (upstream side). Reference points 1u, ("upstream"), 1c ("central plane"), 1d ("downstream"), 2c, and 12c are indicated (cf. Table 1).

2.2 Stereo reconstruction

The data path is identical to that proposed by Soloff *et al.* (1997), except that we use a standard pinhole camera model, with eleven constants to be calibrated for each camera:

$$X = \frac{a_{11}x + a_{12}y + a_{13}z + a_{14}}{a_{31}x + a_{32}y + a_{33}z + 1},$$

$$Y = \frac{a_{21}x + a_{22}y + a_{23}z + a_{24}}{a_{31}x + a_{32}y + a_{33}z + 1} \quad (1)$$

where X *and* Y are image coordinates, and x, y, z are the physical coordinates illustrated in Fig. 2. (The normal to the light sheet is conventionally denoted by z in literature on stereo PIV, but here we use coordinate axes conventional in fluid mechanics). By contrast, Soloff *et al.*'s third-order polynomial mapping function from physical space to image space has 18 constants to be calibrated for each image coordinate, *i.e.* 36 constants for each camera.

We emphasize that the pinhole mapping function (1) can be applied *without modification* to the Scheimpflug arrangement. While this may be obvious to many readers, we have not yet found a straightforward statement of this fact in the SPIV literature. Indeed, a well-known Japanese-language tutorial on SPIV [9] states that "because the lateral magnification varies with position in the image, the geometrical camera model cannot be immediately applied...although in theory it should be possible to introduce the Scheimpflug condition in such a model, no research to date has reported concretely how to do this."

To see that the pinhole model may be applied to a Scheimpflug camera, it suffices to notice that equations (1) contain no reference to a plane of focus (or any other privileged plane such as a light sheet). Consider the "standard" camera in Fig 4 a), in which the lens plane, and thus the plane of focus, are parallel to the image sensor. Point A will be in focus; point B will be out of focus for finite aperture, but neglecting lens aberrations the centroid b of its image can be calculated by the pinhole model. In the Scheimpflug camera shown in b), the lens has been rotated to bring both points A and B into focus, but again neglecting aberrations the positions of their images will be exactly the same as in the standard arrangement. Perhaps confusion has arisen from mistakenly identifying the axis of the lens system with the *optical axis*; the latter being defined as the line passing through the lens center and perpendicular to the image sensor (*i.e.* line *A-a* in Fig4 a) and b)). It is true that in a Scheimpflug camera the optical axis will not in general pass through the center of the sensor, and there is the possibility that the offset of the lens axis from the optical axis will lead to strong image aberration. In our particular setup, this worry turns out to be unfounded; we find that physically collinear points are indeed collinear on the image (to within a pixel), in accord with the pinhole model.

As an ideal check of the validity of the simple pinhole model, and of our stereo reconstruction software, we determined "displacement" vectors

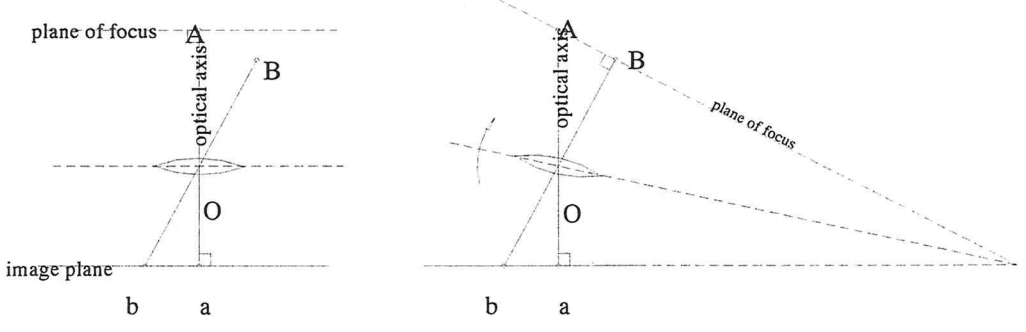

(a) Standard camera (b) Scheimpflug camera

Fig. 4. The pinhole model is equally applicable to standard and Scheimpflug cameras.

between the 12 pairs of points lying at either end of the horizontal rows of 300 μm diameter reference points, and spaced 12 *mm* from each other in the streamwise direction (*e.g.* points *1u* and *1d* in Figs. 2 and 3). The calibration constants a_{ij} were determined from those 24 points and the 12 points in the central plane by a least-squares fit to Eq. 1. Image coordinates were determined to subpixel accuracy by fitting an elliptic Gaussian template. A comparison of the "displacement" components determined from the machining coordinates of the reference points with those found by stereo reconstruction is given in Table 1.

	Coordinates of reference points, mm		Physical separation between upstream and downstream points, mm +/- 0.005 mm			"Displacement" measured by stereo reconstruction, mm		
#	z	y	Δz	Δy	Δx	Δz	Δy	Δx
1	-19.865	37	0.005	0	12	0.02	0.039	11.934
2	0.033	37	0.008	0	12	-0.02	-0.028	12.032
3	20.225	37	0.012	0	12	0.005	-0.038	12.035
4	-19.873	25.333	0.002	0	12	-0.004	-0.021	11.971
5	0	25.333	0.015	0	12	0.033	0.043	11.992
6	20.232	25.333	0.014	0	12	0.016	0	12.042
7	-19.877	13.667	-0.009	0	12	-0.012	-0.051	11.996
8	-0.005	13.667	0.031	0	12	0.039	-0.019	11.975
9	20.23	13.667	0.013	0	12	-0.001	0.003	12.03
10	-19.861	2	0.004	0	12	0.017	0.027	11.956
11	-0.01	2	0.033	0	12	-0.002	0.024	11.927
12	20.219	2	0.015	0	12	0.022	0.002	12.054
			Nondimensional Errors			$\varepsilon_{\Delta z}/\Delta$	$\varepsilon_{\Delta y}/\Delta$	$\varepsilon_{\Delta x}/\Delta$
			Average			-0.00021	-0.00013	-0.00039
			Standard deviation			0.00139	0.00255	0.00362

Table 1. Comparison of the differences in machining coordinates of pairs of reference points with "displacement" components found by stereo reconstruction. Reference points numbers correspond with labels of Figs. 2 and 3. Decimals are omitted from Δy and Δz for readability. Error $\varepsilon_{\Delta z}$ indicates difference between separations in z-direction as measured by SPIV with "true" values as determined by machining coordinates, and similarly for other coordinates.

This comparison experimentally confirms the validity of our calibration procedure and choice of the pinhole mapping function (1). Note that other important sources of error in SPIV are not tested here; registration error is eliminated by assumption, and misalignment of the target in the water channel is not checked. Also, the reference points have a width of three or more pixels on the image, so pixel locking is presumably negligible, which may not be the case with flow tracers.

In the small angle approximation, a planar boundary in refractive index introduces an anisotropic mapping of the object space that cannot, in principle, be described by the pinhole model. The check described above shows that, *under the present experimental conditions,* any errors resulting from this effect are not important. However, it would be well in the future to address this issue theoretically, and to establish clear criteria for neglecting such effects under various conditions. Note that this issue applies equally to a standard camera or a Scheimpflug camera viewing perpendicular through a window into water

3. CROSS-CHECK USING A THIRD CAMERA

We have recently acquired a Pulnix TM-6710 progressive scan camera, capable of 120 *f. p. s.* at a resolution of 680×484 pixels. By performing PIV with a thin, nearly circular laser beam, rather than a laser sheet, and viewing from below through the glass bottom of the water channel, we are now using this third camera ("camera 3") to cross-check the two horizontal velocity components measured by our stereo PIV setup.

Only one of the Nd:YAG lasers is strobed at 30 *Hz* at low pulse energy, at a height of 10 *mm* above the channel bed, and appears in the images of cameras 1 and 2 to be 1.6 *mm* high, and in the images of camera 3 to be 2.0 *mm* wide in the stream direction. Water is supplied at the head of the channel from a hose at a very low flow rate, about 0.25 *liter/sec* in the data reported here, with a flow depth of 10.2 cm. This produces apparently steady secondary flow cells that serve as a useful test case. Fig. 5 shows a comparison of the streamwise and spanwise velocity components as measured from 17 image pairs with Δt = 0.100 sec by SPIV with cameras 1 and 2 (symbols) and by 2C PIV with camera 3 (connected curves). The overall agreement is quite encouraging. To the right of the minimum of streamwise velocity, however, the two measurements differ by up to 0.5 *mm/sec*, or roughly 10% of the velocity there. We are now investigating the cause of this discrepancy.

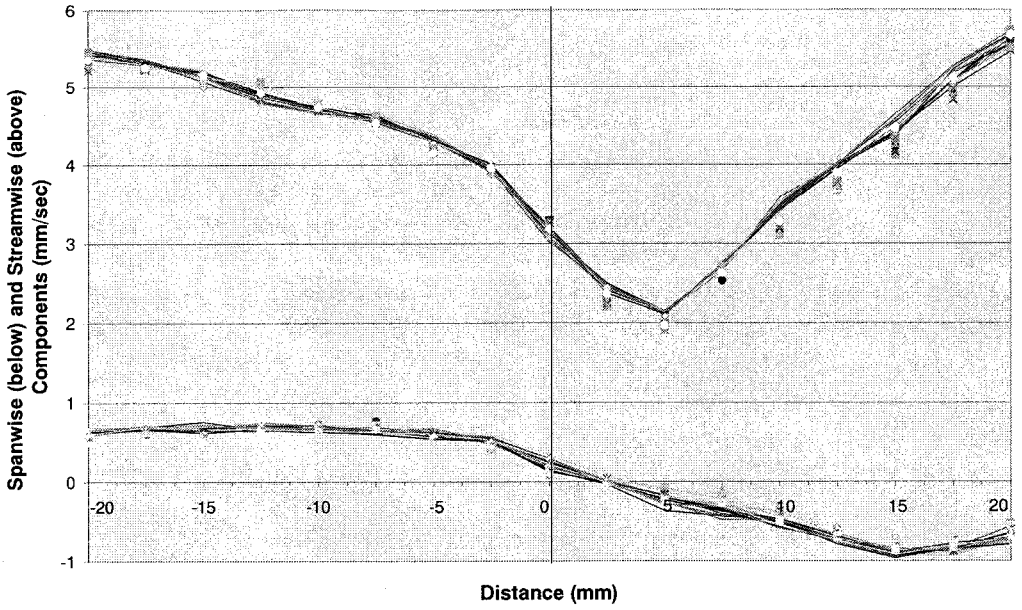

Fig. 5 Simultaneous streamwise (upper graphs) and spanwise (lower graphs) velocity components, from 17 image pairs with Δt = 0.100 sec, by SPIV with cameras 1 and 2 (symbols) and by 2C PIV (connected curves). Horizontal axis is spanwise distance.

4. CONCLUSION

To summarize, we have described a stereo PIV system for time-resolved stereo PIV in the cross-stream plane of an open channel, using Willert's "front-and-rear" camera arrangement[7], and a novel target designed for that arrangement. We have demonstrated, both theoretically and experimentally, the fact that the pinhole camera model can be applied without modification to a Scheimpflug camera if lens aberrations are tolerable. Preliminary results[6] are encouraging qualitatively and, with the exception of the streamwise component, quantitatively insofar as mean values are concerned. We have finally described a stringent cross-check on the stereo PIV results. At the conference, we will report on the results of refined measurements, with the objective of statistically investigating the relation between streamwise vortices, low-speed regions, and regions of high contribution to Reynolds stress. Although the most likely outcome is simply to confirm knowledge already obtained by DNS, we plan in subsequent work to extend our program to higher Reynolds number and to rough boundaries.

ACKNOWLEDGEMENTS

We are grateful for support from the Japanese Ministry of Education, Culture, and Science through a Scientific Grant-in-Aid, and through the Scientific Frontier II Project at Ritsumeikan University. Messrs. Ukai and Himeno, students of the graduate school, assembled the calibration target. Dr. T. Itoh, Mr. K. Matsuki, and Mr. A.T. Nguyen assisted in final preparation of the manuscript. We thank an anonymous referee for pointing out that air-water refraction may invalidate the pinhole model.

REFERENCES

1) Stretch, D., "Automated Pattern Eduction from Turbulent Flow Diagnostics", Center for Turbulence Research Annual Research Briefs, 1990
2) Jeong, J., Hussain, F. Schoppa, W. and Kim, J., "Coherent Structures near the wall in a Turbulent Channel Flow", J. Fluid Mech., Vol. 332, 185-214, 1997
3) Wells, J.C., Yamane, Y., Yamamoto, Y., Egashira, S. and Nakagawa, H., "Dye visualization and P.I.V. analysis of streamwise vorticity structure in a smooth-bed open-channel flow", Annual J. Hydr. Eng., JSCE Vol. 44, 491-496, 2000.
4) Wells, J.C., Yamamoto, Y., Yamane, Y., Egashira, S. and Nakagawa, H., "P.I.V. in the cross-stream plane of a turbulent channel flow: evidence for oblique structure", Proceedings of IUTAM Symposium on Geometry and Statistics of Turbulence, Kambe et al. (eds.), 357-364 (Kluwer), 2001
5) Wells, J.C., Yamamoto, Y., "Experimental spatio-temporal structure of vortical and straining regions near the wall of open-channel flow", Annual J. Hydr. Eng., JSCE Vol. 45, pp. 523-528, 2001
6) Wells, J.C., Kishida, K., "Stereo PIV measurement of near-wall coherent structures in open-channel flow", Annual J. Hydr. Eng., JSCE Vol. 46, pp 523-528, 2002 (in Japanese)
7) Willert, C.E., "Stereoscopic digital particle image velocimetry for application in wind tunnel flows", Meas. Sci Technol. Vol 8, pp. 1465-1479, 1997. See also Raffel, M., Willert, C.E., Kompenhans, J., 1998, "Particle Image Velocimetry", (section 8.3.1) Springer-Verlag. Note that the stereo reconstruction equations make no reference to the orientation of the light sheet.
8) Soloff S.M., Adrian, R.J., Liu, Z.-C., "Distortion compensation for generalized stereoscopic particle image velocimetry for application in wind tunnel flows", Meas. Sci Technol. Vol. 8, pp. 1441-1454, 1997 Fig. 3 gives their recommended data path for SPIV; their recommended mapping function is their equation (18).
9) Nishino, K., "Camera Calibration", 3D PIV, Visualization Society of Japan, VSJ-PIV-S2, pp. 23-39, 1999 (in Japanese).

(Received September 30, 2002)